Title

Retinitis Pigmentosa Mutations in Bad Response to Refrigeration 2 (Brr2) Impair ATPase and Helicase Activity* ♦

Journal

Journal of Biological Chemistry, 291(23)

ISSN

0021-9258

Authors

Ledoux, Sarah
Guthrie, Christine

Publication Date

2016-06-01

DOI

10.1074/jbc.m115.710848

Peer reviewed

THE JOURNAL OF BIOLOGICAL CHEMISTRY VOL. 291, NO. 23, pp. 11954–11965, June 3, 2016

Retinitis Pigmentosa Mutations in Bad Response to Refrigeration 2 (Brr2) Impair ATPase and Helicase Activity*◆

Received for publication, December 15, 2015, and in revised form, March 23, 2016 Published, JBC Papers in Press, April 12, 2016, DOI 10.1074/jbc.M115.710848

Sarah Ledoux and Christine Guthrie[1]

From the Department of Biochemistry and Biophysics, University of California, San Francisco, California 94158

Brr2 is an RNA-dependent ATPase required to unwind the U4/U6 snRNA duplex during spliceosome assembly. Mutations within the ratchet helix of the Brr2 RNA binding channel result in a form of degenerative human blindness known as retinitis pigmentosa (RP). The biochemical consequences of these mutations on Brr2's RNA binding, helicase, and ATPase activity have not yet been characterized. Therefore, we identified the largest construct of Brr2 that is soluble *in vitro*, which truncates the first 247 amino acids of the N terminus (Δ247-Brr2), to characterize the effects of the RP mutations on Brr2 activity. The Δ247-Brr2 RP mutants exhibit a gradient of severity of weakened RNA binding, reduced helicase activity, and reduced ATPase activity compared with wild type Δ247-Brr2. The globular C-terminal Jab1/Mpn1-like domain of Prp8 increases the ability of Δ247-Brr2 to bind the U4/U6 snRNA duplex at high pH and increases Δ247-Brr2's RNA-dependent ATPase activity and the extent of RNA unwinding. However, this domain of Prp8 does not differentially affect the Δ247-Brr2 RP mutants compared with the wild type Δ247-Brr2. When stimulated by Prp8, wild type Δ247-Brr2 is able to unwind long stable duplexes *in vitro,* and even the RP mutants capable of binding RNA with tight affinity are incapable of fully unwinding short duplex RNAs. Our data suggest that the RP mutations within the ratchet helix impair Brr2 translocation through RNA helices.

Introns are removed from pre-mRNA via the precisely coordinated action of the spliceosome, a dynamic ribonucleoprotein complex consisting of five small nuclear (sn) RNAs and over 100 proteins (1, 2). After an intron is identified by the U1 and U2 snRNPs, the U4/U6-U5 triple-snRNP (tri-snRNP)[2] is recruited. The U4/U6 snRNAs, which are held together by both extensive base pairing and protein-RNA interactions, must be unwound so that U4 can be displaced along with the U1 snRNP. After the U2/U6-U5 spliceosome is assembled, splicing catalysis is able to proceed. U4/U6 unwinding is accomplished by Brr2, a large DEIH-ATPase that is part of the U5 snRNP (3). Brr2 must act in a rapid and thorough manner to fully separate the U4 snRNA- and tri-snRNP-specific proteins thus allowing the spliceosome to properly assemble. Additionally, because Brr2 is part of the U5 snRNP and an integral part of the tri-snRNP (4), its activity must be regulated such that U4/U6 unwinding is only able to occur in the context of spliceosome assembly to prevent aberrant tri-snRNP disintegration. After spliceosome assembly, Brr2 remains a part of the spliceosome throughout the two chemical steps of splicing catalysis. Roles for Brr2 activity after spliceosomal activation and during the splicing catalytic pathway have been hypothesized (5–7), indicating that Brr2 regulation must be carefully maintained within the cell.

Brr2 is a large member of the Ski2-like subfamily of superfamily 2 (SF2) ATP-dependent helicases (8, 9). It has a long N-terminal region with predicted unstructured regions and a recently characterized PWI domain (Fig. 1*A*) (10–12). The helicase cassette of Brr2 has a tandem duplication, and only the first domain is catalytically active and able to bind RNA (13, 14). The first helicase cassette is composed of the two RecA domains that are found in all SF2 members and bind ATP and a Sec63 domain that forms one side of the single-stranded RNA binding channel facing the RecA domains (Fig. 1*B*) (4, 14, 15). The Sec63 domain has a ratchet α-helix that has been shown to be important for RNA binding and helicase activity in other SF2 family members (16, 17). However, the importance of the ratchet helix has not yet been characterized for Brr2 RNA helicase and ATPase activity.

Several mutations have been identified within Brr2 that result in a form of autosomal dominant degenerative blindness in humans known as retinitis pigmentosa (18–20). These cluster along the ratchet helix of Brr2's first Sec63 domain and face into the single-stranded RNA binding channel (Fig. 1*C*). Homologous mutations in *Saccharomyces cerevisiae* Brr2 have been shown to have reduced growth in the cold (15 °C) on minimal growth media, when RNA duplexes are more thermodynamically stable and unwinding is expected to be more difficult, as well as reduced tri-snRNP unwinding *in vitro* (18). However, the mechanistic basis of the reduced tri-snRNP unwinding observed *in vitro* is still unclear.

One known regulator of Brr2 activity is Prp8, another large component of the U5 snRNP and a core component of both the tri-snRNP and the assembled spliceosome (4, 12, 21, 22). The globular Jab1/Mpn1-like domain at the C-terminal Prp8 (Prp8(2142–2398)) has been shown to bind to the first helicase cassette of Brr2 (Fig. 1*C*) (4, 15, 23). In multiple turnover helicase assays Brr2 has been shown to be more active in the presence of the C-terminal region of Prp8 (15, 24). However, these experiments were complicated by the fact that they also

* This work was supported by National Institutes of Health Grant GM021119-39 (to C. G.) and American Cancer Society Postdoctoral Fellowship 118703-PF-10-061-01-RMC (to S. L.). The authors declare that they have no conflicts of interest with the contents of this article. The content is solely the responsibility of the authors and does not necessarily represent the official views of the National Institutes of Health.
◆ This article was selected as a Paper of the Week.
[1] American Cancer Society Research Professor of Molecular Genetics. To whom correspondence should be addressed: E-mail: christineguthrie@gmail.com.
[2] The abbreviations used are: tri-snRNP, triple-snRNP; HLH, helix-loop-helix.

included the RNase H-like domain of Prp8 (24), which has been shown to bind to the U4/U6 snRNAs and to occlude the Brr2-binding site (25), as well as the C-terminal tail of Prp8, which has been shown to bind Brr2 directly and prevent Brr2 from binding RNA (23). Additionally, previous experiments performed in the presence of the C-terminal region of Prp8 comprising the RNase H-like domain, Jab1/Mpn1-like domain, and C-terminal tail suggested that Prp8 inhibits Brr2 ATPase activity (24). More recent experiments using only the Jab1/Mpn1-like domain of human form of Prp8 have shown that it does stimulate Brr2 activity in multiple turnover helicase experiments and increases Brr2 ATPase activity (23). The recent findings of how Prp8 influences Brr2 activity make it clear that assumptions about Brr2 activity from previous studies must be re-examined more carefully.

To understand how RP mutations within the ratchet helix of Brr2 affect helicase and ATPase activity, we identified the largest soluble form of recombinant *S. cerevisiae* yeast Brr2, Δ247-Brr2, and tested its activity in a minimal *in vitro* system. Different mutations at the two key positions of the ratchet helix have varied affinities for U4/U6 ranging from wild type affinity to effectively no binding. Helicase reactions reveal that Δ247-Brr2 RP mutants that do bind U4/U6 only unwind a fraction of the total population of duplex RNA despite having similar $K_{½}$ and k_{max} values as the wild type protein. The Δ247-Brr2 RP mutants also had reduced ATPase activity compared with wild type protein. The Jab1/Mpn1-like domain of Prp8 stimulated the ATPase and helicase activity of both the wild type and RP mutant Δ247-Brr2 to a similar degree such that the RP mutant proteins still had reduced activity overall compared with the wild type protein. Overall, our data suggest that the RP mutations in Brr2's ratchet helix affect its interaction with RNA and reduce its ability to translocate through and fully separate the U4/U6 snRNA duplex.

Experimental Procedures

Protein Purification—Truncations of recombinant Brr2 were cloned in a pRS313 plasmid driven by an overexpressing glyceraldehyde-3-phosphate dehydrogenase promoter and transformed into S288C cells endogenously expressing WT Brr2. Cells were grown at 30 °C to a final A_{600} of 4 in single drop-out −HIS minimal media to preserve the presence of the plasmid. IgG-Sepharose FastFlow beads (GE Healthcare) were used to purify the C-terminal tandem affinity purification-tagged protein. After tobacco etch virus cleavage of the protein A tag, the eluate was loaded onto a calmodulin-agarose (Sigma) column for a secondary purification. The purification was performed as described previously (24) with the addition of a Complete EDTA-free protease inhibitor tablet (Roche Applied Science) and 1 mM leupeptin in the lysis buffer. Peak eluted fractions were identified using SDS-PAGE and were dialyzed twice for 2 h against Buffer A (20 mM HEPES (pH 7.9), 200 mM NaCl, 0.2 mM EDTA, 20% glycerol, and 5 mM β-mercaptoethanol).

Prp8(2142–2398) was cloned with an N-terminal His_6 tag and transformed into Rosetta (DE3)pLysS cells (Novagen). Cultures were grown in LB media at 37 °C to an A_{600} of 0.4, cooled to 16 °C, and induced with 1 mM isopropyl 1-thio-β-D-galactopyranoside (Sigma). After 16 h, cells were harvested and lysed via sonication in the presence of 1 mM benzamidine, 0.5 mM PMSF, and a Complete EDTA-free protease inhibitor tablet (Roche Applied Science). Prp8(2142–2398) was purified according to the protocol for native protein purification in the QIAexpressionist handbook (Qiagen). Peak eluted fractions were identified using SDS-PAGE and were dialyzed twice for 2 h against Buffer A.

RNA Preparation—U4 and U6 snRNAs were synthesized via run-off transcription of pUC19 plasmids using the Thermo Fisher Scientific T7 Megascript transcription kit and protocol. U6 was transcribed with a mixture of [γ-^{32}P]UTP (PerkinElmer Life Sciences) and UTP according to the Megascript protocol. Model duplex RNAs were either purchased from IDT (for lengths <20 nucleotides) or transcribed from overlapping DNA primers containing a T7 promoter sequence. Transcribed RNAs were purified via separation on 6% (w/v) 29:1 TBE polyacrylamide gels under denaturing conditions. RNA was extracted from the gel using electroelution followed by ethanol precipitation. Model duplex top strand RNA was treated with calf intestinal phosphatase (New England Biolabs) to remove the 5′-terminal phosphate and incubated with T4 polynucleotide kinase (New England Biolabs) and [γ-^{32}P]ATP (PerkinElmer Life Sciences) according to protocol from New England Biolabs. RNAs were hybridized at high concentrations in 15 mM HEPES (pH 7.9) and 400 mM NaCl by heating to 75 °C for 5 min after which $MgCl_2$ was added to a final concentration of 10 mM, and samples were allowed to cool and refold on ice. Duplex RNA was then diluted with water to a working concentration of 10 nM for RNA binding and helicase assays.

EMSA—For each experiment, fresh 50% serial dilutions of Brr2 were made using Buffer A. A final concentration of 0.5 nM U4/U6 was incubated for 5 min with the various concentrations of Brr2 at 30 °C to allow binding to equilibrate unless otherwise noted in the text. Final reaction conditions were 40 mM HEPES (pH 7.0), 30 mM NaCl, 2 mM $Mg(OAc)_2$, 1 mM DTT (0.9%/trace glycerol). The final reaction conditions take into account the salt carried over from both the protein dialysis buffers and RNA hybridization buffer. Samples were then loaded onto cold 4% 79:1 native TBE polyacrylamide gels and run at 170 V for 20 min to separate free U4/U6 from Brr2-bound U4/U6. Gels were exposed to phosphorimager screens (Molecular Dynamics) overnight. The fraction of Brr2-bound U4/U6 was quantified using ImageQuant software. The equilibrium dissociation constant was calculated by plotting the fraction protein-bound U4/U6 *versus* protein concentration using the equation K_d = ([Brr2] [U4/U6])/[Brr2-U4/U6]. Reactions using Prp8(2142–2398) used equimolar amounts of Brr2 and Prp8 that were allowed to pre-bind in dilution buffer prior to the addition of U4/U6.

Helicase Assay—U4/U6 with ^{32}P body-labeled U6 was incubated to a final concentration of 0.5 nM with 250 nM Brr2 with or without equimolar Prp8(2142–2398) at 30 °C. Reactions were performed in final conditions identical to those used for performing EMSAs. Reactions were initiated by addition of a final concentration of 4 mM ATP/$Mg(OAc)_2$. For model duplex reactions, ATP was mixed with 5 μM unlabeled oligonucleotide $poly(U)_{20}$ single-stranded RNA trap to prevent re-initiation and multiple turnover reactions. Individual time points were

quenched by mixing 10 μl of the reaction with 4 μl of quenching buffer (50 mM EDTA (pH 8.0), 500 mM NaCl, 2.5% SDS). The products of U4/U6 helicase reactions were separated using cold 9% native TBE 29:1 polyacrylamide gels run at 170 V for 30 min to separate free U6 from U4/U6. Gels were exposed to phosphorimager screens overnight. The fraction of free U6 at each time point was calculated using ImageQuant software and the rate of helicase was quantified using fraction unwound = U4/U6•(1 − exp(−k_{app}•time)). Reactions using model duplex RNAs were performed similarly with the exceptions that the shorter strand was 5′ end-labeled ^{32}P, and the reaction products were separated on a 15% 29:1 polyacrylamide gels.

Co-pulldown Assay—Co-pulldown assays were performed using His_6-tagged Prp8(2142–2398) and untagged Brr2 proteins. Prp8(2142–2398) was immobilized on nickel-nitrilotriacetic acid paramagnetic beads (Thermo Scientific). Unbound protein in the supernatant was removed by multiple washes with the EMSA reaction buffer. A constant 1 nM concentration of Brr2 was incubated with 50% serial dilutions of Prp8(2142–2398) ranging from 400 to 1.5 nM. Unbound supernatants were concentrated and run on 3–8% Tris acetate SDS-PAGE (Life Technologies, Inc.). Gels were stained using Krypton stain (Thermo Scientific) and analyzed by Typhoon imaging and ImageQuant analysis.

ATPase Assay—Multiple turnover ATPase assays were performed using 1 μl of 3000 Ci/mmol [α-^{32}P]ATP (PerkinElmer Life Sciences) diluted into 100 μl of 1 mM cold ATP/$Mg(OAc)_2$. Final reaction conditions were 40 mM HEPES (pH 7.0), 30 mM NaCl, 2 mM $Mg(OAc)_2$, and 1 mM DTT. 50 nM Brr2 and 500 nM dark U4/U6 were incubated for 5 min at 30 °C before the addition of the ATP mixture. Aliquots were quenched in 500 mM EDTA at each time point before spotting on PEI-cellulose TLC plates (Sigma) that had been pre-run in water. After drying, 2 μl of the quenched reaction was spotted on the plates and allowed to dry before reaction products were separated using 0.3 M potassium phosphate (pH 7.6). TLC plates were exposed to phosphorimager screens overnight. The fraction of hydrolyzed ADP to total signal at each time point was calculated using ImageQuant software.

Results

N-terminal Truncations Identify Minimal Brr2 in Vitro Construct—Expression of full-length Brr2 from *S. cerevisiae* results in significant aggregation, making it difficult to isolate the high concentrations of soluble Brr2 that are necessary for single turnover biochemical experiments. To determine the longest optimal *in vitro* construct of Brr2, we cloned and purified several truncated forms of the protein based on sequence conservation and the predicted structured regions of the N terminus. A version of Brr2 with a minimal truncation beginning at the first predicted structured region (Δ113) was insoluble at high concentrations. This truncation has already been shown to be conditionally lethal in *S. cerevisiae* and impedes spliceosome assembly *in vivo*, but it does not eliminate Brr2's helicase activity in purified tri-snRNPs (26). A similar truncation has also recently been shown to be prone to aggregation by Wahl and co-workers (11). A high resolution structure of the N terminus of Brr2 in the tri-snRNP is still lacking. The aggregation exhibited by the full-length Brr2 and Δ113-Brr2 (Fig. 1*A*) *in vitro* suggests that the N-terminal region may require a binding partner to be properly structured.

We also expressed a version of Brr2 containing the recently characterized PWI-like domain (Δ247-Brr2) (Fig. 1*A*) (10). The truncation site was chosen based on the predicted PWI domain (27) and phylogenetic sequence homology. The largest truncation we tested encompassed the entire N terminus of Brr2, which is overall less conserved than the helicase cassettes (Δ422-Brr2) (Fig. 1*A*). Crystal structures of the complete N-terminal truncation form of Brr2 have been solved for both the yeast and human protein and demonstrate that both helicase cassettes are stably folded and active *in vitro* in the absence of the N-terminal region (14, 15). Although the Δ247-Brr2 and Δ422-Brr2 truncations would be lethal *in vivo* (26), cells grown with the recombinant protein expressed in the presence of untagged full-length wild type (WT) Brr2 did not have a dominant negative growth phenotype. Unlike full-length Brr2 or Δ113-Brr2, proteins with either the Δ247 or Δ422 N-terminal truncation were completely soluble *in vitro* at high concentrations. Interestingly, similar truncated forms of yeast and human Brr2 were recently identified by the Wahl and co-workers (11) that showed similar improvements in solubility compared with longer forms of the protein *in vitro*.

A native gel mobility shift assay was employed to determine whether either Δ247 or Δ422 N-terminal truncation affected Brr2's affinity for U4/U6. Transcribed U4 snRNA was hybridized to ^{32}P body-labeled U6 to form the U4/U6 snRNA duplex (Fig. 1*D*). 50% serial dilutions of Brr2 were made using Buffer A at pH 7.0 and were incubated with the U4/U6 reaction mixture for 5 min to allow binding to equilibrate. U4/U6 bound by Brr2 was then separated from free U4/U6 using native 4% PAGE at 4 °C (Fig. 2*A*). Both Brr2 N-terminal truncation constructs have similar affinity for U4/U6 (Δ422-Brr2 K_d = 35.6 ± 2.7; Δ247-Brr2 K_d = 19.5 ± 5.3); therefore, the longer version of Brr2 (Δ247-Brr2) containing the PWI domain was chosen for further study.

In homologous helicases of Brr2 the ratchet helix has been shown to contact the single strand of nucleic acid that helicases track along as they unwind duplex regions (16, 17). Several mutations associated with the human disease RP that results in degenerative blindness are found within the ratchet helix of Brr2's catalytically active first helicase cassette. These mutants are found on the ratchet helix along the α-helical face oriented toward the RNA binding channel (18). The position of the mutations suggest they may affect either the affinity of Brr2 for RNA or the ability of Brr2 to translocate through an RNA duplex. To characterize the effects RP mutations have on Brr2 activity, we made three RP mutations within our truncated recombinant yeast Δ247-Brr2 construct as follows: N1104L, R1107A, and R1107L. We determined the affinity of the RP mutants for U4/U6 and found that N1104L has an affinity identical to WT Brr2 (Fig. 2*B* and Table 1). However, both mutations at position 1107 weakened the RNA affinity compared with WT. Mutating the conserved arginine at position 1107 to a small uncharged alanine resulted in a 3-fold reduction in affinity. Mutating Arg-1107 to a bulky uncharged leucine resulted in a greater than 25-fold loss in affinity resulting in a K_d value that

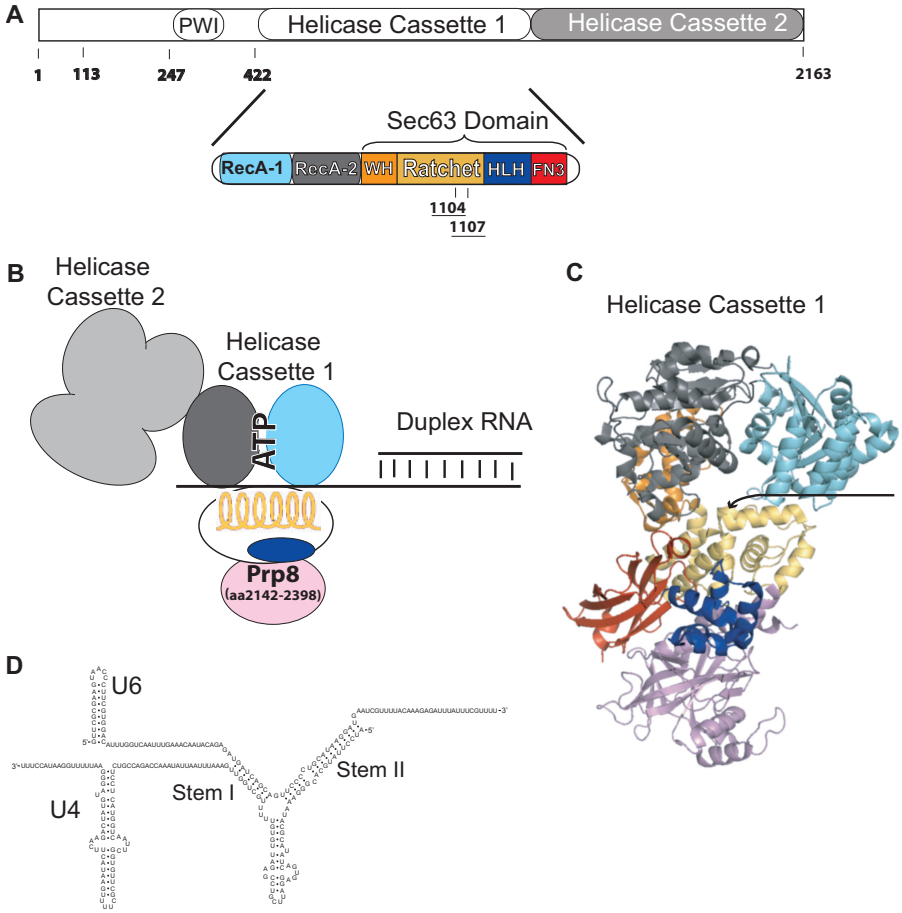

FIGURE 1. **RP mutations are found in the ratchet helix of Brr2's helicase cassette 1.** *A,* schematic diagram of the Brr2 primary structure. The amino acid number of N-terminal truncations tested are shown *below* the diagram. Helicase cassette 1 is the catalytically active helicase region with its sub-domains shown in the color-coded zoom-in diagram. RecA-1 is shown in *teal* and RecA-2 in *dark gray*. The Sec63-like domain is composed of several sub-domains as follows: the Winged Helix domain (*WH*) is shown in *orange*; Ratchet domain is shown in *gold*; HLH domain is shown in *blue*; and Fibronectin3-like domain (FN3) is shown in *red*. The amino acid positions of the RP mutations 1104 and 1107 are shown *below* the ratchet domain. *B,* schematic depiction of domain structure of helicase cassettes 1 and 2 color-coded the same as in *A*. ATP binds between the two RecA domains, and the single-stranded region of RNA passes between the RecA domains and Ratchet domain. It is unknown how the N-terminal region of Brr2, including the PWI domain, interacts with the helicase cassettes. The globular Jab1/Mpn-like domain of Prp8 interacts with the Sec63 domain of helicase cassette 1. *C,* crystal structure of helicase cassette 1 interacting with the globular Jab1/Mpn-like domain of Prp8 Protein Data Bank code 4BGD color-coded similarly as above and oriented as in *B*. A *black arrow* follows above the ratchet helix and the path of the single-stranded RNA binding channel and points between positions 1104 and 1107 on the ratchet helix. *D,* sequence and secondary structure of the U4/U6 snRNA duplex.

was too high to accurately determine under our reaction conditions (Fig. 2*B* and Table 1).

The globular Jab1/Mpn1-like domain of Prp8 (amino acids 2142–2398) has previously been shown to bind the first helicase domain of Brr2 in the helix-loop-helix (HLH) domain (Fig. 1*C*) near the exit of the RNA binding channel (15, 23). The Jab1/Mpn1-like domain of human Prp8 has recently been shown to stimulate Brr2's helicase activity (23), although its effects on Brr2's RNA binding affinity remain untested. The final C-terminal 16 amino acids of Prp8(2399–2413) form a tail that has been implicated in repressing Brr2 helicase activity by occluding the RNA binding channel (23, 28). Experiments performed on Brr2 in the presence of the entire C terminus of Prp8, including both the globular Jab1/Mpn1-like domain and C-terminal tail in addition to the RNase H-like domain of Prp8, give variable results depending on the ratio of RNA, Brr2, and Prp8 used (23, 24, 28). These variable results likely indicate competition between the stimulatory properties of the Jab1/Mpn1-like domain and the inhibitory properties of the C-terminal tail and RNase H-like domain. At high concentrations of Prp8, it is likely that the C-terminal inhibitory tail may bind the Brr2 RNA binding channel and block the U4/U6 snRNAs from binding. Also, the RNase H-like domain may directly bind U4/U6 and prevent Brr2 from binding its substrate. Therefore, for clarity of data interpretation, only the stimulatory globular Jab1/Mpn1-like domain was used for these experiments. Recent work has shown that the Jab1/Mpn1-like domain has a tight binding affinity of ~10 nM for Brr2 (28). To determine whether the globular Jab1/Mpn1-like domain, Prp8(2142–2398), would either affect the WT Brr2 affinity for U4/U6 or increase the RP mutant Δ247-Brr2 affinity to WT levels, we repeated the EMSAs in the presence of equimolar Prp8(2142–2398). The presence of Prp8(2142–2398) did not affect the affinity of WT or RP mutant Δ247-Brr2 for U4/U6 (Table 1) and did not bind U4/U6 in the absence of Brr2 (Fig. 2*B*). In addition, the WT and RP mutant Δ247-Brr2 proteins all had comparable affinities for Prp8(2142–2398) determined via a co-pulldown assay (Table 1) that are similar to previously reported WT measurements (28).

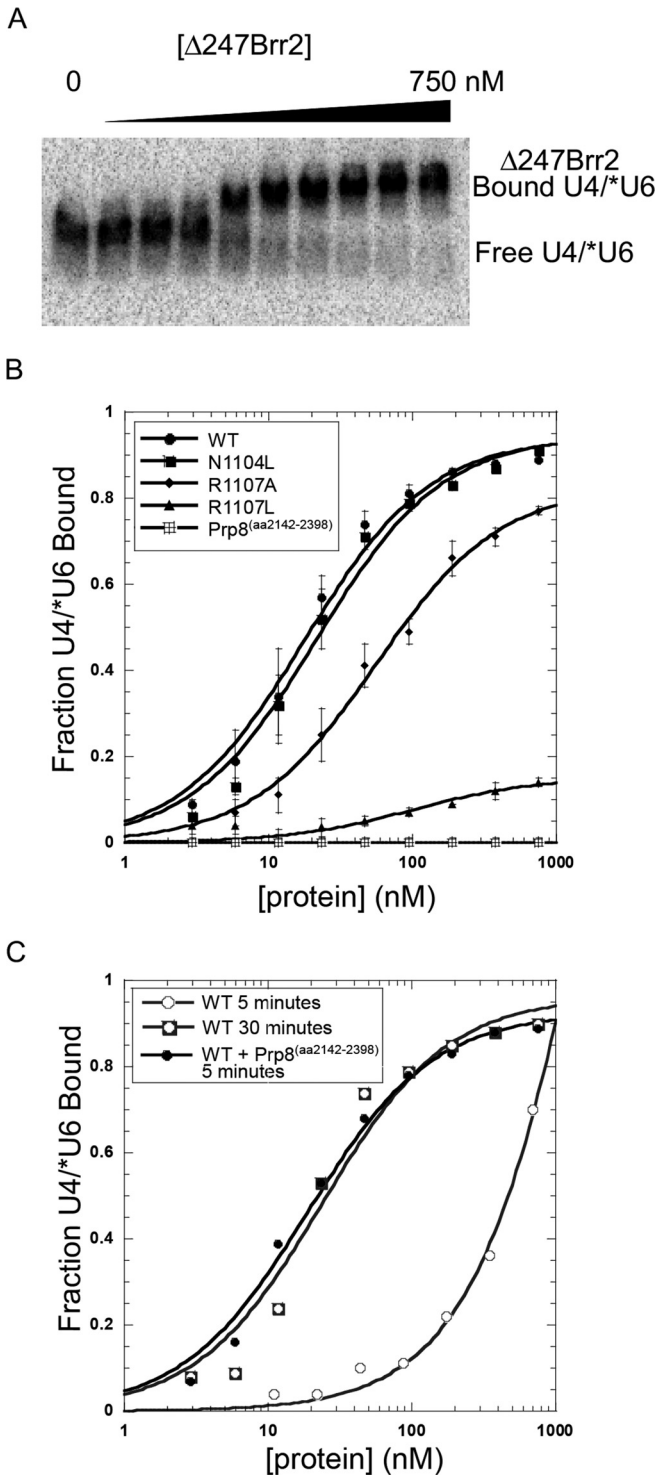

FIGURE 2. **RP mutations weaken Δ247-Brr2 affinity for U4/U6.** *A,* representative raw data of 4% native TBE 79:1 polyacrylamide gel depicting an electrophoretic mobility shift assay with WT Δ247-Brr2 and U4/U6 using ^{32}P-body-labeled U6. *B,* fraction of U4/U6 bound by Brr2 at each protein concentration at pH 7.0 was calculated *versus* the total radioactive signal. Three independent experiments were averaged, and the standard error of the mean is represented by *error bars*. *Circles,* WT Δ247-Brr2; *squares,* Δ247-Brr2(N1104L); *diamonds,* Δ247-Brr2(R1107A), and *triangles,* Δ247-Brr2-(R1107L). *C,* representative data showing WT Δ247-Brr2 fully binds U4/U6 faster at pH 7.9 when in the presence of Prp8(2142–2398). *Open circles,* WT Δ247-Brr2 incubated with U4/U6 for 5 min; *filled circles,* WT Δ247-Brr2 in the presence of equimolar Prp8(2142–2398) incubated with U4/U6 for 5 min; *boxed circles,* WT Δ247-Brr2 incubated with U4/U6 for 30 min before separating on native gel.

This indicates that the RP mutations do not affect Brr2 interaction with Prp8(2142–2398). Thus, the stimulatory effect observed for Prp8(2142–2398) on Brr2's unwinding activity is not simply due to increasing Brr2's affinity for U4/U6.

Prp8(2142–2398) Increases the Rate of U4/U6 Binding by Brr2 at High pH—Interestingly, we did uncover a role for Prp8(2142–2398) in influencing Brr2 RNA binding affinity in a pH-dependent manner. WT and RP mutant Δ247-Brr2 both bound U4/U6 *in vitro* quickly at pH 7.0 but required longer incubation times to fully bind RNA when the pH was raised to pH 7.9 (Fig. 2*C*). However, when Prp8(2142–2398) was present under the higher pH conditions, Δ247-Brr2 was able to bind U4/U6 within a short 5-min incubation time, similar to Δ247-Brr2 alone at neutral pH. Effects on helicase activity and pH have been observed for other helicases and could be due to increased flexibility of the protein allowing the RNA binding channel to open more easily at reduced pH levels (29). This suggests that Prp8(2142–2398) may play a role in allowing access of U4/U6 to Brr2's RNA binding channel.

Despite being a viable mutation in both humans and *S. cerevisiae*, the R1107L RP mutation is correlated to an earlier age of onset of blindness in humans and more reduced yeast growth at cold temperature than the N1104L RP mutation (18, 19, 30). The weak binding exhibited by Δ247-Brr2(R1107L) for U4/U6 suggests that the *in vivo* phenotypes may be due at least partially to reduced interactions with the U4/U6 snRNA duplex we observed *in vitro*. Because the Δ247-Brr2(R1107L) does not have a tight enough binding affinity for U4/U6 to create saturated binding conditions for our helicase and ATPase assays, it was excluded from further experiments (Fig. 2*B*).

Prp8(2142–2398) Increases the Extent of Δ247-Brr2's Helicase Activity—To test the effect of the RP mutations on Δ247-Brr2's RNA unwinding activity, we performed helicase assays using the U4/U6 snRNA duplex. A saturating concentration of Δ247-Brr2 was incubated with the hybridized U4/U6 snRNAs for 5 min at 30 °C to allow full protein binding to occur. The helicase reaction was initiated by the addition of ATP/$Mg(OAc)_2$. Aliquots were withdrawn and quenched at set time points after which the hybridized U4/U6 was separated from the fully unwound ^{32}P-labeled U6 on cold native 9% polyacrylamide gels (Fig. 3*A*).

WT Δ247-Brr2 only unwinds ~50% of the population of U4/U6 duplexes (Fig. 3*B*). Interestingly, the unwinding curve shows a lag in time before unwound free labeled U6 is observed. This suggests that there is a hidden kinetic step in addition to the unwinding rate, possibly caused by the highly structured U4/U6 snRNA duplex. Although the RP mutant Δ247-Brr2 proteins bind U4/U6 snRNA duplexes with similar affinity to the WT protein, they do not unwind any measurable amount of the duplexes in the absence of Prp8(2142–2398). This indicates that the tight binding of the RP mutant Δ247-Brr2 to RNA either results in a non-productive conformation or that the RP mutation reduces Brr2's processive ability to unwind the U4/U6 duplex to completion, allowing the partially unwound duplexes to re-hybridize or migrate on the polyacrylamide gel as fully hybridized RNA. Because only completely separated RNA strands are visualized as being unwound in the all-or-

TABLE 1

Binding affinity of WT and Δ247-Brr2 RP for RNA and Prp8(2142–2398)

Values are the average of at least three independent experiments with the standard error of the mean shown.

Δ247-Brr2 construct	K_d of Brr2 alone for U4/U6	K_d of Brr2 + Prp8(2142–2398) for U4/U6	K_d of Brr2 for Prp8(2142–2398)
	nM	nM	nM
WT	19.5 ± 5.3	26.2 ± 3.3	8.17 ± 0.38
N1104L	22.7 ± 5.3	57.5 ± 18	9.77 ± 2.6
R1107A	61.4 ± 20	51.8 ± 8.6	8.54 ± 0.94
R1107L	>500	>500	12.0 ± 2.6

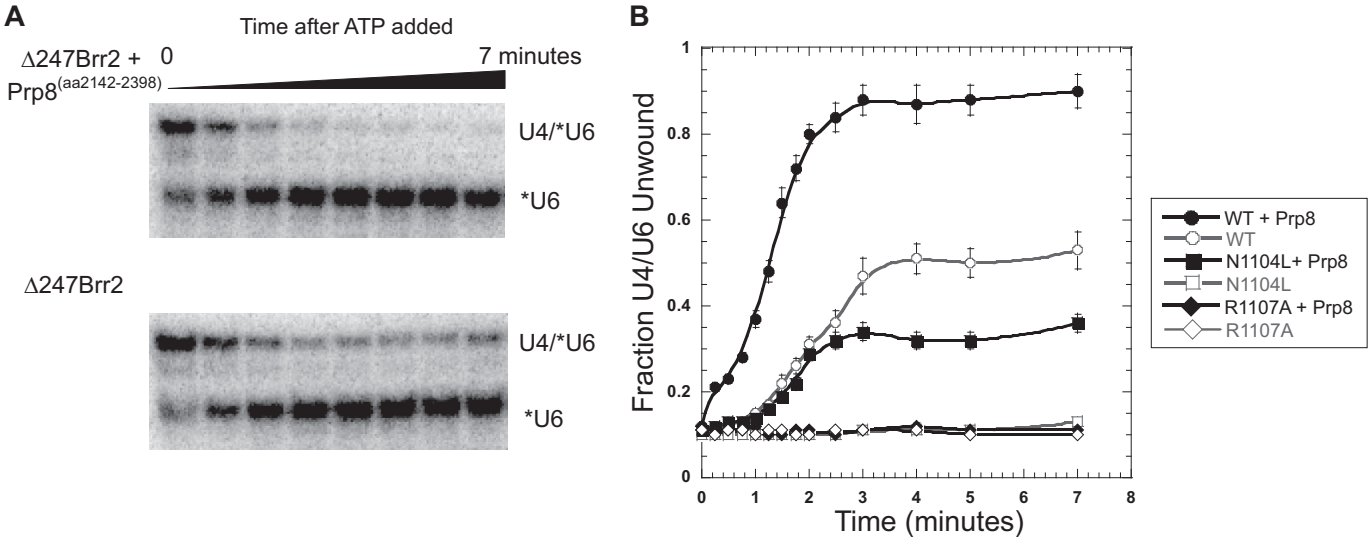

FIGURE 3. **RP mutations and absence of Prp8(2142–2398) reduce Δ247-Brr2 helicase activity on U4/U6.** *A,* representative raw data of 9% native TBE 29:1 polyacrylamide gel showing U4/U6 unwinding over time visualized using ^{32}P-body-labeled U6. *Top,* WT Δ247-Brr2 with equimolar Prp8(2142–2398). *Bottom,* WT Δ247-Brr2 alone. *B,* fraction of free U6 compared with the total radioactive signal at each time point was determined. Average data from at least three separate experiments for each sample is shown with a *connecting line. Error bars* represent the standard error of the mean. *Circles,* WT Δ247-Brr2; *squares,* Δ247-Brr2(N1104L), and *diamonds,* Δ247-Brr2(R1107A). *Filled black symbols* represent experiments performed in the presence of equimolar Prp8(2142–2398), and *open gray symbols* represent experiments performed with Brr2 alone.

nothing gel-based assay, partial unwinding is not observable in our assay.

When Prp8(2142–2398) is present, WT Δ247-Brr2 is able to unwind the total population of U4/U6 rapidly and to completion (Fig. 3*B*). The lag phase of the unwinding curve is also reduced. This suggests that Prp8(2142–2398) either enables Brr2 to form a productive complex with the RNA or stimulates it processive motion along the U4/U6 duplex. Although Prp8(2142–2398) did not affect the affinity of Δ247-Brr2 for U4/U6 at neutral pH, the fact that it can influence U4/U6 binding at higher pH suggests that it may modulate the interaction of Brr2 with U4/U6 during the helicase reaction.

Interestingly, the ability of the N1104L and R1107A RP mutants to unwind U4/U6 in the presence of Prp8(2142–2398) under saturating U4/U6 binding conditions varied despite their similar affinity for RNA. Although Δ247-Brr2(R1107A) only exhibits a 3-fold reduction in affinity for the U4/U6 snRNA duplex compared with WT or Δ247-Brr2(N1104L), it was not able to unwind any detectable amount of U4/U6 duplex (Fig. 3*B*). Also, despite the fact that Δ247-Brr2(N1104L) has the same affinity for U4/U6 as WT Δ247-Brr2, it was only able to unwind about 35% of the population of U4/U6 duplexes even in the presence of Prp8(2142–2398). This amounts to a lower fraction of the U4/U6 snRNA duplex population able to be fully unwound by the RP mutant Δ247-Brr2(N1104L) stimulated by Prp8(2142–2398) than for the WT Δ247-Brr2 without the stimulation of Prp8(2142–2398). The RP mutations within the Brr2 ratchet helix may be affecting Brr2's ability to either productively contact RNA or to translocate on it in a manner that cannot be overcome by the stimulation of Prp8(2142–2398).

RP Mutants Have ATPase Defects Even When Stimulated by Prp8(2142–2398)—To determine whether the RP mutants within the RNA binding channel also influence ATPase activity, we compared the ATPase activity of the WT Δ247-Brr2 to the RP mutant Δ247-Brr2s in the presence and absence of both U4/U6 and Prp8(2142–2398). A mixture of [α-^{32}P]ATP and unlabeled ATP/Mg(OAc)$_2$ was reacted with the protein at 30 °C under multiple turnover conditions. Aliquots were removed at set time points and quenched in 500 mM EDTA. ADP was separated from ATP via TLC on PEI-cellulose plates in 0.3 M potassium phosphate (pH 7.6) (Fig. 4*A*). As demonstrated previously, Brr2 has maximal ATPase activity in the presence of both RNA (24) and Prp8's globular Jab1/Mpn-like domain (23). In the absence of U4/U6 RNA, the ATPase activity of WT Δ247-Brr2 was negligible, whereas the ATPase activity in the presence of U4/U6 but absence of Prp8(2142–2398) was substantial (Fig. 4*B*). Interestingly, despite the fact that the RP mutations are in the ratchet helix of the RNA binding channel and not the ATP binding cleft of Brr2, the RP mutant ATPase activity correlates exactly with helicase activity. Δ247-Brr2(N1104L) shows a level of ATPase activity when stimulated by Prp8(2142–2398) that is similar to the WT Δ247-Brr2 alone.

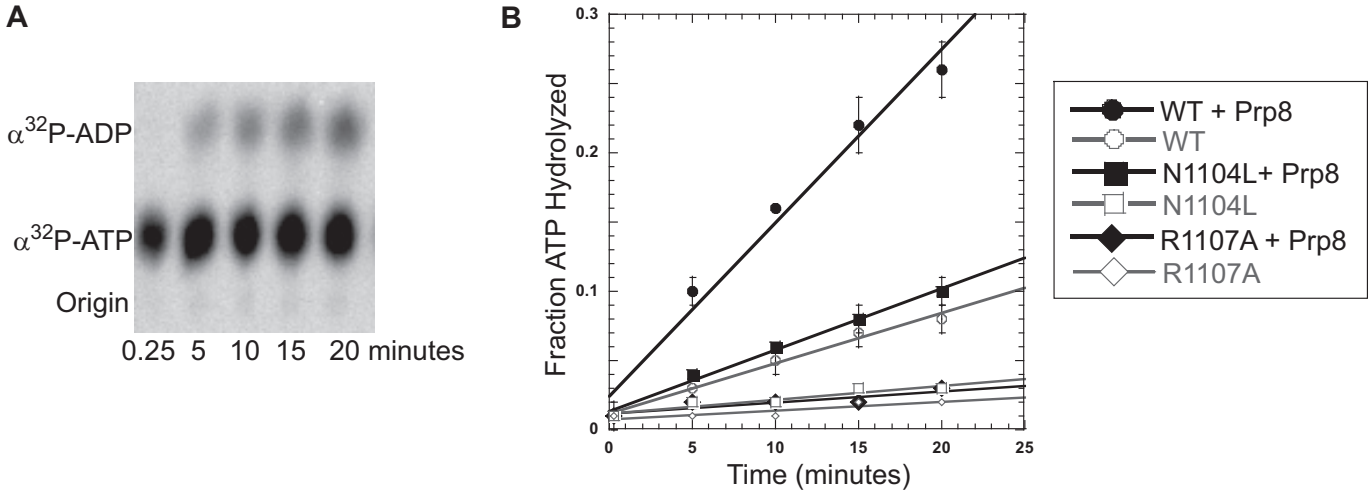

FIGURE 4. **RP mutations and absence of Prp8(2142–2398) reduce Δ247-Brr2 ATPase activity.** *A,* representative raw data of ATPase time course performed using WT Δ247-Brr2 and Prp8(2142–2398). Time points were quenched in 500 mM EDTA, spotted on a PEI-cellulose TLC plate, and run in 0.3 M potassium phosphate (pH 7.6) to separate hydrolyzed ADP from ATP. *B,* fraction of ATP hydrolyzed was calculated based on the amount of ADP compared to total radioactive signal at each time point. Three independent experiments were averaged, and the standard error of the mean is represented by *error bars*. *Filled black symbols* represent experiments performed in the presence of equimolar Prp8(2142–2398), and *open gray symbols* represent experiments performed with Brr2 alone. *Circles,* WT Δ247-Brr2; *squares,* Δ247-Brr2(N1104L), and *diamonds,* Δ247-Brr2(R1107A).

The other Δ247-Brr2 RP mutants exhibit only background levels of ATPase activity even in the presence of Prp8(2142–2398). This indicates that ATP hydrolysis is coordinated with RNA binding or translocation. It might have been expected that significantly more ATP would be hydrolyzed in repeated attempts to translocate and unwind the RNA duplex with the RP mutants; however, this is obviously not the case.

Single Turnover Model Duplex Unwinding—The U4/U6 duplex structure is complex and contains a three-way junction between the Brr2-binding site on U4 *in vivo* and Stem II (Fig. 1*D*). Also, because Brr2 is a directional 3′ → 5′-helicase (25), in the minimal *in vitro* system Brr2 could presumably bind initially to the 3′ end of U6 or unwind stem loops of U4 that would be occluded by other bound proteins *in vivo*. RNA structural rearrangements could also be responsible for the lag phase observed in Prp8-free helicase assays (Fig. 3*B*). Therefore, to simplify our observations, we used model RNA duplexes to further examine differences between the WT and RP mutant Δ247-Brr2 proteins with and without Prp8(2142–2398) (Fig. 5*A*). These duplexes contain a 3′ 22-nucleotide single-stranded overhang of computationally predicted low intra-helix forming potential followed by a perfectly base-paired duplex of varying length. The sequence of the single-stranded region was chosen from the U4 3′ end in the region where Brr2 is predicted to bind (5). The model 17 base-paired long duplex is based on the Stem II region of U4/U6 (Fig. 1*D*) but is perfectly base-paired.

The model 17-mer RNA duplex was used in single turnover helicase assays. The 17-nucleotide ^{32}P 5′ end-labeled top strand was hybridized to the 5′ end of a longer bottom strand with perfect complementarity for a calculated melting temperature of ~52 °C (Fig. 5*A*). A poly(U)$_{20}$ single-stranded RNA was added along with ATP/Mg(OAc)$_2$ when the reaction was initiated as a trap to bind any free Δ247-Brr2 and to prevent rebinding and multiple cycles of helicase activity on the labeled duplex RNAs. Unwound top strand RNA was separated from the duplex RNA using cold 15% native PAGE (Fig. 5*B*). Single exponential rate curves fit to the data using the model duplex do not show the lag phase observed with full-length U4/U6 (Fig. 3*B*), suggesting the lag was caused by the complex structured RNA and not due solely to Brr2 helicase activity. However, as with the helicase assays using the full-length U4/U6, Δ247-Brr2 alone only unwinds a portion of the total fraction of duplex RNAs (Fig. 5*C*). Also, the RP mutant Δ247-Brr2 by itself does not unwind any measurable amount of duplex.

Similar to the full-length U4/U6, the presence of Prp8(2142–2398) results in the WT Δ247-Brr2 unwinding the total population of duplex RNA nearly to completion (Fig. 5*C*). Table 2 shows the fraction of the population of RNA duplexes unwound, represented as the final amplitude of the helicase reaction. The N1104L RP mutant Δ247-Brr2 is able to unwind ~35% of the model duplex RNA in the presence of Prp8(2142–2398), similar to the level of unwinding exhibited with full-length U4/U6 snRNA duplexes. Interestingly, unlike helicase reactions performed with full-length U4/U6 duplexes, WT Δ247-Brr2 unwinds a lower extent of the population of model 17-mer RNA duplexes than the RP mutant Δ247-Brr2(N1104L) (Fig. 5*C*). This may reveal an added stimulatory effect by Prp8(2142–2398) necessary on the minimal model duplex that is masked by proper structure or sequence effects present with the full-length U4/U6 snRNAs.

The $K_{½}$ and k_{max} values of unwinding the model 17-mer RNA duplex were determined by measuring the apparent rate of helicase activity at increasing concentrations of Δ247-Brr2 and fitting the data to the Michaelis-Menten isotherm (Fig. 5*D*). Despite unwinding different extents of the overall population of RNA duplexes, the maximal rate of activity is similar for the WT Δ247-Brr2 both with and without the stimulation of Prp8(2142–2398) and also for the RP mutant Δ247-Brr2(N1104L) when stimulated by Prp8(2142–2398) (Table 2). This suggests that Δ247-Brr2 unwinds the small fraction of the total population of duplex RNAs that is active on similar rates, and it is only the extent of the reaction that is affected by the

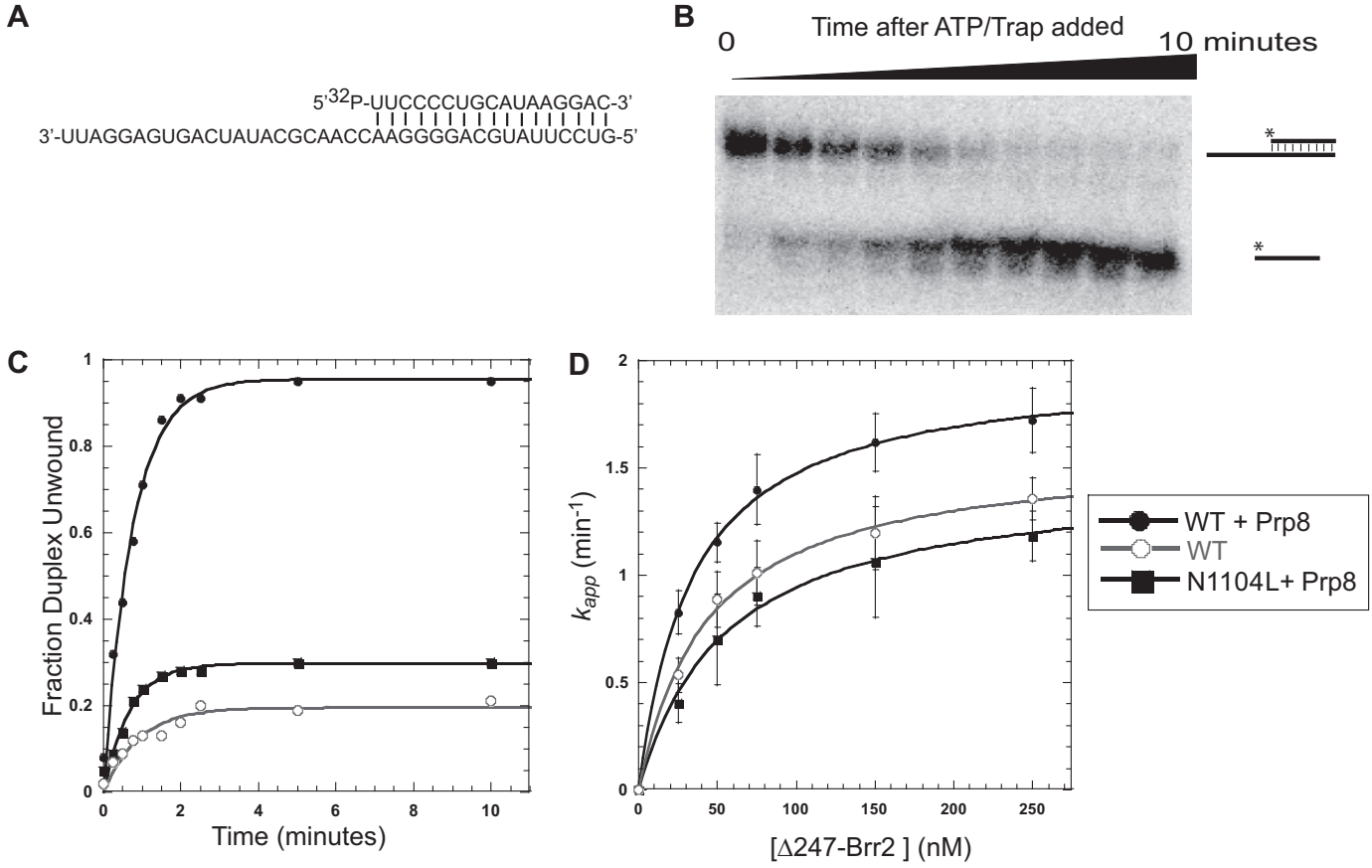

FIGURE 5. **Despite unwinding a higher extent of duplexes, WT and RP mutant Δ247-Brr2 have similar Prp8(2142–2398)-stimulated $K_{1/2}$ and k_{max}.** *A,* model 17-mer duplex sequence. Short top strand is labeled with a 5′ radioactive phosphate. *B,* representative raw data of 15% native TBE 29:1 polyacrylamide gel depicting model duplex unwinding assay. The shorter top strand was phosphorylated with ^{32}P for visualization. *C,* fraction of model 17-mer duplex unwound at each time point was calculated by the amount of free top strand *versus* total radioactive signal. *Filled black symbols* represent experiments performed in the presence of equimolar Prp8(2142–2398), and *open gray circles* represent experiments performed with Brr2 alone. *Circles,* WT Δ247-Brr2; *squares,* Δ247-Brr2(N1104L). *D,* apparent rates determined from *B* were plotted against protein concentration to determine the $K_{1/2}$ and k_{max}. Three independent experiments for each protein concentration were averaged, and the standard error of the mean is represented by *error bars*.

TABLE 2

Kinetic parameters for WT *versus* RP mutant Δ247-Brr2 activity on model 17-mer duplex

Values are the average of at least three independent experiments with the standard error of the mean shown. ND means not determined.

	Model 17-mer $K_{1/2}$	Model 17-mer k_{max}	Model 17-mer amplitude of fraction unwound
	nM	*min*$^{-1}$	
WT + Prp8(2142–2398)	34.2 ± 2.0	1.98 ± 0.033	0.91 ± 0.02
N1104L + Prp8(2142–2398)	55.0 ± 7.5	1.46 ± 0.070	0.35 ± 0.04
R1107A + Prp8(2142–2398)	ND	ND	0.20 ± 0.02
WT alone	43.9 ± 4.5	1.5 ± 0.051	0.14 ± 0.02

presence of an RP mutation or Prp8(2142–2398). The population of duplex RNAs that cannot be unwound could either be due to a lack of Brr2 productively engaging with the RNA or a reduction in the ability of Brr2 to translocate fully through the RNA duplexes.

Δ247-Brr2 Can Unwind Long Model Duplex RNAs—To test whether the difference in the fraction of RNA duplexes unwound observed between WT and RP mutant Δ247-Brr2 is due to the overall length of duplex each protein is able to unwind, we tested the helicase activity of each protein on model duplexes of increasing length (Fig. 6*A*). Even in the presence of Prp8(2142–2398), the extent of duplex unwound by WT Δ247-Brr2 begins to drop quickly as the length of the duplex region increases (Fig. 6*B*). However, WT Δ247-Brr2 is still able to unwind a notable fraction of the population of RNA duplexes 40 bp in length. This is a duplex significantly longer than either any stem in U4/U6 or any known natural RNA duplex, which suggests Brr2 has the inherent capability to be very processive for an RNA helicase. In the context of the tri-snRNP, when Brr2, Prp8, and the RNA are all carefully held in a productive orientation, it is possible that Brr2 may be even more processive than when isolated *in vitro*.

In contrast, either the Δ247-Brr2 in the absence of Prp8(2142–2398) stimulation or the RP mutant Δ247-Brr2 stimulated by Prp8(2142–2398) was unable to unwind the entire population of even very short model duplexes (Fig. 6*B*). Helicase reactions using the model 14-mer duplex resulted in a larger extent of unwinding than was observed on the model

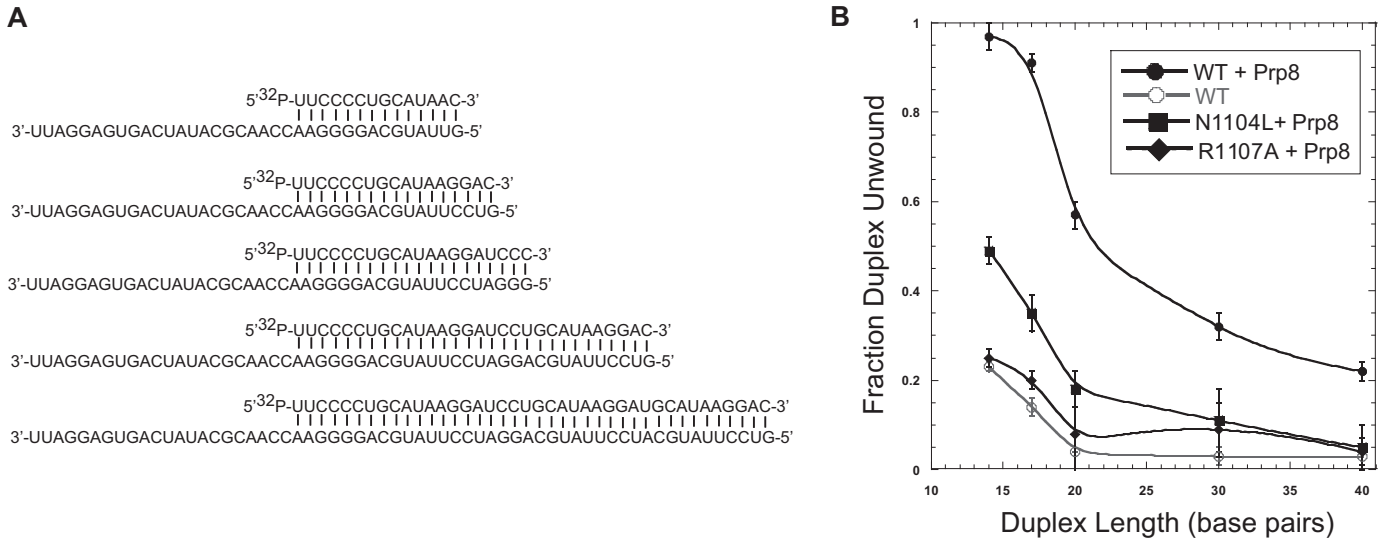

FIGURE 6. **Δ247-Brr2 unwinds a lower extent of duplexes as number of base pairs increases.** *A,* sequence of model duplexes used. Only the sequence at the blunt end of the duplex region was altered to exclude differences of interactions with the single-stranded/duplex junction. *B,* final amplitude of unwinding for each length of model duplex is plotted (and shown with *connecting lines* between each point). Three independent experiments were averaged, and the standard error of the mean is represented by *error bars*. *Filled black symbols* represent experiments performed in the presence of equimolar Prp8(2142–2398), and *open gray symbols* represent experiments performed with Brr2 alone. *Circles,* WT Δ247-Brr2; *squares,* Δ247-Brr2(N1104L), and *diamonds,* Δ247-Brr2(R1107A).

17-mer RNA duplex, but the RP mutant Brr2 was still unable to unwind the entire population of duplex RNA. The model 14-mer duplex has a lower predicted melting temperature than the model 17-mer duplex (T_m 40 °C *versus* 52 °C) and a shorter distance for Brr2 to have to translocate to completely displace the shorter RNA strand. The fact that the RP mutant Brr2 cannot fully unwind the entire population of even short duplex RNAs emphasizes the importance of the wild type residues in Brr2's ratchet helix on it helicase activity. The overall extent of unwinding for each of the model duplexes drops to no duplexes unwound as the length of the base-paired region increases. This leaves open the possibility that RP mutant Δ247-Brr2 forms a non-productive complex incapable of helicase activity on some RNA duplexes. Alternatively, the RP mutations may reduce Brr2's helicase processivity, thus impairing the ability of Brr2 to take the multiple translocation steps required to achieve complete duplex strand dissociation.

Discussion

RP mutations resulting in degenerative human blindness have been previously identified in the ratchet helix of Brr2's single-stranded RNA binding channel (Fig. 1, *A–C*). Although human blindness and yeast cold-sensitive growth phenotypes are associated with these mutations (18–20), a mechanistic explanation for how these mutations impair Brr2 activity has been lacking. Here we have shown that, despite having similar binding affinities for the U4/U6 snRNA duplex as WT Δ247-Brr2, RP mutations within the ratchet helix result in reduced ATPase activity and a lower fraction of the RNA duplex population being fully unwound. Binding of the Prp8(2142–2398) globular Jab1/Mpn1-like domain does not affect the affinity of Δ247-Brr2 for U4/U6 (Table 1), although at high pH values it increases the speed of Δ247-Brr2 binding to RNA (Fig. 2*C*). This suggests that Prp8(2142–2398) may affect Brr2 conformational dynamics allowing RNA access to Brr2. Previous research has suggested that the C-terminal region of Prp8 increases Brr2 affinity for the U4/U6 snRNAs (31). However, the region of Prp8 used previously included the RNase H-like domain of Prp8, which has been shown to bind the U4/U6 snRNAs (25) and was likely the cause of the increase in U4/U6 snRNA binding by the proteins. Prp8(2142–2398) stimulates the helicase activity of Δ247-Brr2 with a similar magnitude for the WT protein and the RP mutant Δ247-Brr2, indicating that stimulation of Prp8 cannot overcome the defect incurred by mutating the Brr2 ratchet helix. The RP mutations in the Brr2 ratchet helix result in a reduced fraction of the population of RNA duplexes unwound compared with WT Brr2. The RP mutations at position 1107 exhibited more severe mechanistic defects in all assays performed than the mutation at position 1104. Taken together, these results suggest that mutations within the ratchet helix impair the Brr2 interaction with and translocation through RNA duplexes.

In SF2 helicases that possess a ratchet domain, the ratchet α-helix is proposed to not only bind the single-stranded nucleic acid but to also help pull it through the nucleic acid binding channel as the helicase translocates and separates the base-paired nucleic acid region. In Brr2, the ratchet helix has recently been shown to contact the middle region of the U4 snRNA as the tracking strand of RNA (4). In this structure, the asparagine at position 1104 of Brr2 is within hydrogen bonding distance of the nitrogen at position 7 of the adenine base at position 80 of the U4 snRNA. The arginine is not within hydrogen bonding distance of the RNA and may be acting as an electrostatic shield for the highly negative RNA backbone. Structures of the close homolog Hel308 bound to DNA (16) and the Ski2-like subfamily member Mtr4 bound to RNA (17) show a range of interactions between the ratchet helix and oligonucleotide are possible. Mtr4 has been shown to have similar phenotypes when its ratchet helix is mutated in positions corresponding to the RP

mutations in Brr2 (17). Interestingly, the severity of phenotypes is inverted compared with Brr2 with respect to the position of the mutations along the ratchet helix. In *S. cerevisiae*, Mtr4 mutations at the first position along the ratchet helix Arg-1030, akin to position Asn-1104 in Brr2, have more deleterious effects compared with mutations at the second position Glu-1033, akin to position Arg-1107 in Brr2. Although analogous positions along the ratchet helix in Mtr4 and Hel308 have been structurally shown to interact directly with the nucleic acid, both proteins have different conserved amino acids in each position that result in different types of nucleic acids interactions. The analogous region in the ratchet helix of Hel308 uses tryptophan to form base-stacking interactions with its bound DNA (16), whereas the Mtr4 ratchet helix residues form hydrogen bonds with its bound RNA (17). The interactions between the Brr2 ratchet helix and U4 RNA could affect either the binding or movement of RNA through the Brr2 RNA binding channel as U4/U6 snRNAs are unwound during spliceosome assembly.

WT Brr2 is able to unwind long duplexes of RNA when stimulated by Prp8(2142–2398) (Fig. 6*B*) despite the fact that long, perfectly complementary RNA duplexes are not found in the spliceosome. If Brr2's role in spliceosome assembly is to unwind the U4/U6 snRNA duplex, then the longest perfectly base-paired region it encounters is only 11 base pairs long after the mismatch nucleotide bulge in Stem II. In the absence of Prp8(2142–2398) stimulation, Brr2 does not fully unwind a large fraction of U4/U6 molecules or model 14-mer RNA duplexes to completion *in vitro*. Thus, Prp8(2142–2398) stimulation is necessary to ensure that Brr2 efficiently performs its unwinding task to completion, which is necessary *in vivo* to ensure that spliceosome assembly proceeds correctly. In the context of the tri-snRNP, Brr2 and U4/U6 are held in alignment by many other proteins (4, 12, 22), and a notable increase in the rate of tri-snRNP unwinding compared with Brr2 unwinding U4/U6 alone has been observed (18). Additional contacts with the proteins and RNAs in the tri-snRNP may be provided by the N-terminal 247 amino acids that were truncated in our experiments to enable purification of soluble Brr2 *in vitro*.

Prp8(2142–2398) stimulation increases the overall extent of total duplex unwound, but does not significantly affect the K_d, $K_{½}$, or k_{max} values of the reaction at neutral pH (Tables 1 and 2). Because the effect of Prp8(2142–2398) is a similar magnitude for both the WT and reduced activity of the RP mutant Brr2, it is clear that Prp8's stimulation is not sufficient to overcome defects within the Brr2 ratchet helix. This suggests that Prp8(2142–2398) may aid the processivity of Brr2, preventing it from dissociating from U4/U6 before the duplex is fully unwound without directly affecting the interaction of Brr2 with RNA. Alternatively, the role of Prp8(2142–2398) may be to alter the conformation of Brr2 to enable it to form a productive complex with RNA capable of efficient translocation. Importantly, even in the context of stimulation by Prp8(2142–2398), the RP mutants reduce the activity of Brr2 possibly by causing conformational constraints that trap Brr2 in a non-productive conformation that is able to bind RNA but cannot translocate efficiently on it.

Interestingly, Prp8(2142–2398) does increase the ability of Brr2 to bind to U4/U6 at higher pH. The Prp8 Jab1/Mpn-like domain has been shown crystallographically to bind to the HLH domain of Brr2 near the exit of the RNA binding channel (Fig. 1*C*) (15, 23). The overall structure of Brr2 is similar in both the free and Jab1/Mpn-like domain-bound structures (14, 15, 23). The recent cryo-electron microscopy structure of the yeast tri-snRNP shows that the U4 snRNA exits Brr2 in a region close to where the Prp8 Jab1/Mpn1-like domain binds to the Brr2 HLH domain (4). It is possible that the binding of the Jab1/Mpn1-like domain may affect the flexibility of this region of Brr2. In fact, Brr2's HLH domain is predicted to be flexible due to its high B factor in the yeast crystal structure (15). A similar domain is present in Hel308 and has been proposed to influence helicase activity, acting like a molecular brake on the DNA and interacting with the ratchet helix (32, 33). Prp8 may function to aid in the flexibility of Brr2's HLH domain during RNA binding or during the exit of RNA out of Brr2 as it is being progressively unwound. The only other member of the Ski2-like subfamily of helicases to possess an HLH domain is Slh1 (9), a transcription-associated helicase with a tandem helicase cassette repeat and PWI domain in the N-terminal region predicted from the primary sequence. However, biochemical and structural data for Slh1 are still lacking. Other members of the Ski2-like subfamily lack an HLH domain and instead have an Arch domain insertion that is not found in Brr2 (9). The presence of the HLH domain makes Brr2 more similar in some ways to the DNA helicase Hel308 (16) than to Mtr4 or Ski2 despite the presence of the ratchet helix in all of these proteins.

Interestingly, in addition to positively regulating Brr2 by stimulating its helicase (24) and ATPase activity (23, 28), Prp8 has also been shown to negatively regulate Brr2. The C-terminal 16 amino acids of Prp8 form a negatively charged tail that is able to bind into the RNA binding channel of Brr2 thus blocking the binding of RNA to Brr2 (23, 28). Negative regulation of Brr2 may be necessary because Brr2 is able to unwind a significant fraction of RNA duplexes even in the absence of Prp8(2142–2398) stimulation. Therefore, because Brr2 has an inherent intermediate level of helicase activity, to be fully active Brr2 cannot simply be de-repressed but must be additionally stimulated. Such a tunable range of activity may be necessary because Brr2 is associated with its U4/U6 snRNA substrates as part of the tri-snRNP and must be prevented from separating the duplex prematurely when not associated with a pre-mRNA as part of spliceosome assembly. The recent cryo-electron microscopy structure of the yeast tri-snRNP shows that Brr2 is able to bind the single-stranded region of U4 outside of the context of the assembling spliceosome (4). It is also been shown that the yeast tri-snRNP will disassemble upon addition of ATP even in the absence of a pre-mRNA (3, 34), thus demonstrating the need to repress premature helicase activity of Brr2. However, once the spliceosome begins to assemble, Brr2 must act efficiently to fully separate and displace the U4 snRNA, which is not part of the assembled active spliceosome. To completely separate the duplexed U4/U6 snRNAs as well as the proteins that are bound to them, Brr2 may need to be stimulated above its basal level of activity. Because Brr2 remains a part of the catalytically active spliceosome throughout the pre-mRNA

splicing cycle, it may need to be repressed again to prevent it from binding part of the RNA catalytic core of the spliceosome and prematurely dissociating the spliceosome. Interestingly, several RP mutants have also been identified in the C-terminal tail of Prp8 that weaken Prp8's repression of Brr2 activity by weakening the binding interaction between the two proteins (28, 35, 36). Thus, RP disease can be caused either by Brr2 not being fully active or by Brr2 not being fully repressed, thus emphasizing the importance of properly regulating Brr2 helicase activity.

The ratchet helix mutations studied here had a gradation of phenotypic severity that was similar in every assay. The N1104L mutation results in the most WT-like mechanistic phenotype followed by the R1107A mutation and with the R1107L mutation having the most severe defect in that it did not bind the U4/U6 duplex well under the conditions tested (Fig. 2*B*). *In vivo* growth assays have also suggested that position 1104 within the ratchet helix tolerates mutations more readily than at position 1107 (18). The homologous position to yeast Asn-1104 in humans is a serine, thus conserving the hydroxyl group and implicating its importance in a possible hydrogen bonding interaction with bound RNA. Position 1107 is universally conserved in Brr2, and we have shown here that when it is mutated to a much smaller alanine residue it greatly reduces the Brr2 ATPase and helicase activity, although it is still able to bind RNA. However, when position 1107 is mutated to a bulky hydrophobic leucine, the protein loses its ability to bind RNA (Fig. 2*B*). This suggests that the hydrophobic bulk of leucine may sterically occlude the RNA binding channel.

The RP mutations within Brr2's ratchet helix have an exacerbated defect *in vitro* compared with *in vivo* data in yeast and humans. Although the R1107L mutant was unable to bind RNA appreciably *in vitro* in the minimal system tested here, *in vivo* this mutant only exhibits reduced yeast growth at cold temperatures when the RNA duplex would be further thermodynamically stabilized (18). In *S. cerevisiae* the N1104L mutant only exhibits a slight growth defect at low temperature in minimal growth media (18). Although *in vitro* biochemical assays cannot replicate the full complexity of the *in vivo* environment, it is striking that the trends of both the *in vitro* mechanistic experiments and the *in vivo* phenotypes correlate. For example, the age of onset for vision loss in humans is younger for people with the R1107L mutation (19) compared with the mutation at position 1104 (30), indicating a stronger phenotype.

The fact that the mechanistic phenotypes observed with the minimal *in vitro* system are more severe than even the tri-snRNP unwinding rates measured *in vitro* (18) suggests that other tri-snRNP proteins function to stabilize and position Brr2's interactions with the U4/U6 snRNAs. The recent cryo-electron microscopy structure of the tri-snRNP shows that Brr2 interacts with the U4 snRNA while being positioned by Prp8 (4, 34). The U4 and U6 snRNAs are similarly held in place by a number of other proteins as well as different regions of Prp8 (4, 12, 22). These protein-protein and protein-RNA interactions may act to mask the serious defects that the purified recombinant RP mutant Δ247-Brr2 has with RNA binding, ATPase activity, and RNA duplex unwinding to completion.

Although our results show the importance of the ratchet helix for Brr2 RNA-dependent ATPase and helicase activity, many interesting questions remain open. Fully understanding the nature of how Brr2 is regulated by the stimulation and repression by Prp8 and the mechanism by which the ratchet helix interacts with RNA as it moves through the Brr2 RNA binding channel will be necessary to fully understand the mechanism of the RP mutations. It will be interesting in the future to tease apart whether the RP mutants are affecting Brr2's ability to form a productive complex on the RNA capable of the conformational dynamics necessary for translocation or whether they are reducing Brr2's processivity of unwinding fully through duplex RNAs.

Author Contributions—S. L. designed and performed the experiments. S. L. and C. G. wrote the manuscript.

Acknowledgments—We thank C. Maeder and members of the Guthrie lab for helpful discussions and critical reading of the manuscript.

References

1. Wahl, M. C., Will, C. L., and Lührmann, R. (2009) The spliceosome: design principles of a dynamic RNP machine. *Cell* **136,** 701–718
2. Will, C. L., and Lührmann, R. (2011) Spliceosome structure and function. *Cold Spring Harb. Perspect. Biol.* **3,** a003707
3. Raghunathan, P. L., and Guthrie, C. (1998) RNA unwinding in U4/U6 snRNPs requires ATP hydrolysis and the DEIH-box splicing factor Brr2. *Curr. Biol.* **8,** 847–855
4. Nguyen, T. H., Galej, W. P., Bai, X. C., Oubridge, C., Newman, A. J., Scheres, S. H., and Nagai, K. (2016) Cryo-EM structure of the yeast U4/U6.U5 tri-snRNP at 3.7 Å resolution. *Nature* **530,** 298–302
5. Hahn, D., Kudla, G., Tollervey, D., and Beggs, J. D. (2012) Brr2p-mediated conformational rearrangements in the spliceosome during activation and substrate repositioning. *Genes Dev.* **26,** 2408–2421
6. Bellare, P., Small, E. C., Huang, X., Wohlschlegel, J. A., Staley, J. P., Sontheimer, E. J. (2008) A role for ubiquitin in the spliceosome assembly pathway. *Nat. Struct. Mol. Biol.* **15,** 444–451
7. Small, E. C., Leggett, S. R., Winans, A. A., and Staley, J. P. (2006) The EF-G-like GTPase Snu114p regulates spliceosome dynamics mediated by Brr2p, a DExD/H box ATPase. *Mol. Cell* **23,** 389–399
8. Fairman-Williams, M. E., Guenther, U.-P., Jankowsky, E. (2010) SF1 and SF2 helicases: family matters. *Curr. Opin. Struct. Biol.* **20,** 313–324
9. Johnson, S. J., and Jackson, R. N. (2013) Ski2-like RNA helicase structures: common themes and complex assemblies. *RNA Biol.* **10,** 33–43
10. Absmeier, E., Rosenberger, L., Apelt, L., Becke, C., Santos, K. F., Stelzl, U., and Wahl, M. C. (2015) A noncanonical PWI domain in the N-terminal helicase-associated region of the spliceosomal Brr2 protein. *Acta Crystallogr. D Biol. Crystallogr.* **71,** 762–771
11. Absmeier, E., Wollenhaupt, J., Mozaffari-Jovin, S., Becke, C., Lee, C.-T., Preussner, M., Heyd, F., Urlaub, H., Lührmann, R., Santos, K. F., and Wahl, M. C. (2015) The large N-terminal region of the Brr2 RNA helicase guides productive spliceosome activation. *Genes Dev.* **29,** 2576–2587
12. Agafonov, D. E., Kastner, B., Dybkov, O., Hofele, R. V., Liu, W.-T., Urlaub, H., Lührmann, R., and Stark, H. (2016) Molecular architecture of the human U4/U6.U5 tri-snRNP. *Science* **351,** 1416–1420
13. Kim, D. H., and Rossi, J. J. (1999) The first ATPase domain of the yeast 246-kDa protein is required for *in vivo* unwinding of the U4/U6 duplex. *RNA* **5,** 959–971
14. Santos, K. F., Jovin, S. M., Weber, G., Pena, V., Lührmann, R., and Wahl, M. C. (2012) Structural basis for functional cooperation between tandem helicase cassettes in Brr2-mediated remodeling of the spliceosome. *Proc. Natl. Acad. Sci. U.S.A.* **109,** 17418–17423
15. Nguyen, T. H., Li, J., Galej, W. P., Oshikane, H., Newman, A. J., and Nagai, K. (2013) Structural basis of Brr2-Prp8 interactions and implications for

U5 snRNP biogenesis and the spliceosome active site. *Structure* **21,** 910–919
16. Büttner, K., Nehring, S., and Hopfner, K.-P. (2007) Structural basis for DNA duplex separation by a superfamily-2 helicase. *Nat. Struct. Mol. Biol.* **14,** 647–652
17. Taylor, L. L., Jackson, R. N., Rexhepaj, M., King, A. K., Lott, L. K., van Hoof, A., and Johnson, S. J. (2014) The Mtr4 ratchet helix and arch domain both function to promote RNA unwinding. *Nucleic Acids Res.* **42,** 13861–13872
18. Zhao, C., Bellur, D. L., Lu, S., Zhao, F., Grassi, M. A., Bowne, S. J., Sullivan, L. S., Daiger, S. P., Chen, L. J., Pang, C. P., Zhao, K., Staley, J. P., and Larsson, C. (2009) Autosomal-dominant retinitis pigmentosa caused by a mutation in SNRNP200, a gene required for unwinding of U4/U6 snRNAs. *Am. J. Hum. Genet.* **85,** 617–627
19. Li, N., Mei, H., MacDonald, I. M., Jiao, X., and Hejtmancik, J. F. (2010) Mutations in ASCC3L1 on 2q11.2 are associated with autosomal dominant retinitis pigmentosa in a Chinese family. *Invest. Ophthalmol. Vis. Sci.* **51,** 1036–1043
20. Benaglio, P., McGee, T. L., Capelli, L. P., Harper, S., Berson, E. L., and Rivolta, C. (2011) Next generation sequencing of pooled samples reveals new SNRNP200 mutations associated with retinitis pigmentosa. *Hum. Mutat.* **32,** E2246–E2258
21. Yan, C., Hang, J., Wan, R., Huang, M., Wong, C. C., and Shi, Y. (2015) Structure of a yeast spliceosome at 3.6-angstrom resolution. *Science* **349,** 1182–1191
22. Wan, R., Yan, C., Bai, R., Wang, L., Huang, M., Wong, C. C., and Shi, Y. (2016) The 3.8 Å structure of the U4/U6.U5 tri-snRNP: Insights into spliceosome assembly and catalysis. *Science* **351,** 466–475
23. Mozaffari-Jovin, S., Wandersleben, T., Santos, K. F., Will, C. L., Lührmann, R., and Wahl, M. C. (2013) Inhibition of RNA helicase Brr2 by the C-terminal tail of the spliceosomal protein Prp8. *Science* **341,** 80–84
24. Maeder, C., Kutach, A. K., and Guthrie, C. (2009) ATP-dependent unwinding of U4/U6 snRNAs by the Brr2 helicase requires the C terminus of Prp8. *Nat. Struct. Mol. Biol.* **16,** 42–48
25. Mozaffari-Jovin, S., Santos, K. F., Hsiao, H.-H., Will, C. L., Urlaub, H., Wahl, M. C., and Lührmann, R. (2012) The Prp8 RNase H-like domain inhibits Brr2-mediated U4/U6 snRNA unwinding by blocking Brr2 loading onto the U4 snRNA. *Genes Dev.* **26,** 2422–2434
26. Zhang, L., Li, X., Hill, R. C., Qiu, Y., Zhang, W., Hansen, K. C., and Zhao, R. (2015) Brr2 plays a role in spliceosomal activation in addition to U4/U6 unwinding. *Nucleic Acids Res.* **43,** 3286–3297
27. Korneta, I., Magnus, M., and Bujnicki, J. M. (2012) Structural bioinformatics of the human spliceosomal proteome. *Nucleic Acids Res.* **40,** 7046–7065
28. Mozaffari-Jovin, S., Wandersleben, T., Santos, K. F., Will, C. L., Lührmann, R., and Wahl, M. C. (2014) Novel regulatory principles of the spliceosomal Brr2 RNA helicase and links to retinal disease in humans. *RNA Biol.* **11,** 298–312
29. Ventura, G. T., Costa, E. C., Capaccia, A. M., and Mohana-Borges, R. (2014) pH-dependent conformational changes in the HCV NS3 protein modulate its ATPase and helicase activities. *PLoS One* **9,** e115941
30. Zhao, C., Lu, S., Zhou, X., Zhang, X., Zhao, K., and Larsson, C. (2006) A novel locus (RP33) for autosomal dominant retinitis pigmentosa mapping to chromosomal region 2cen-q12.1. *Hum Genet.* **119,** 617–623
31. Zhang, L., Xu, T., Maeder, C., Bud, L.-O., Shanks, J., Nix, J., Guthrie, C., Pleiss, J. A., and Zhao, R. (2009) Structural evidence for consecutive Hel308-like modules in the spliceosomal ATPase Brr2. *Nat. Struct. Mol. Biol.* **16,** 731–779
32. Richards, J. D., Johnson, K. A., Liu, H., McRobbie, A.-M., McMahon, S., Oke, M., Carter, L., Naismith, J. H., and White, M. F. (2008) Structure of the DNA repair helicase hel308 reveals DNA binding and autoinhibitory domains. *J. Biol. Chem.* **283,** 5118–5126
33. Woodman, I. L., Briggs, G. S., and Bolt, E. L. (2007) Archaeal Hel308 domain V couples DNA binding to ATP hydrolysis and positions DNA for unwinding over the helicase ratchet. *J. Mol. Biol.* **374,** 1139–1144
34. Nguyen, T. H., Galej, W. P., Bai, X.-C., Savva, C. G., Newman, A. J., Scheres, S. H., and Nagai, K. (2015) The architecture of the spliceosomal U4/U6.U5 tri-snRNP. *Nature* 523, 47–52
35. Pena, V., Liu, S., Bujnicki, J. M., Lührmann, R., and Wahl, M. C. (2007) Structure of a multipartite protein-protein interaction domain in splicing factor prp8 and its link to retinitis pigmentosa. *Mol. Cell* **25,** 615–624
36. Grainger, R. J., and Beggs, J. D. (2005) Prp8 protein: At the heart of the spliceosome. *RNA* **11,** 533–557